

Monte Carlo Calculation of the Free Energy of Simple Cubic Lattice Random Walks

Marc L. Mansfield*

Michigan Molecular Institute, 1910 W. St. Andrews Road, Midland, Michigan 48640

Karan P. Singh

Department of Mathematics, Central Michigan University,
Mount Pleasant, Michigan 48859. Received December 15, 1988;
Revised Manuscript Received February 15, 1989

ABSTRACT: We have computed, using umbrella sampling techniques, the free energy of Domb-Joyce simple cubic lattice walks over the complete range of excluded-volume interaction $0 \leq w \leq 1$ for walks of varying length $10 \leq N \leq 500$. The partition function is well represented over the entire range of w and N by the expression $ay^N N^{\gamma-1}$, where a , y , and γ are functions of w . The function $a(w)$ is near 1 for all w but could not be computed too precisely. The function $\alpha(w) = \gamma - 1$ is 0 for $w = 0$ and increases through the cross-over region to an asymptotic value of about 0.18 at larger w . The connectivity constant, $y(w)$, decreases monotonically from 6 at $w = 0$ to about 4.68 at $w = 1$ and was computed quite precisely.

Introduction

The Domb-Joyce model¹ of lattice random walks has the following Hamiltonian:

$$H = \sum_{i < j} \delta_{ij} \epsilon = c \epsilon \quad (1)$$

where δ_{ij} is 1 if the i th and j th beads of the walk occupy the same lattice site and 0 if they do not; c , therefore, is the total number of such pairwise contacts in the chain; and ϵ is the energy per contact. We also define the parameter

$$w = 1 - e^{-\beta \epsilon} \quad (2)$$

Defined in this way, $(1 - w)^c$ is the statistical weight of a chain with c pairwise contacts; w changes from 0 to 1 as we go from ideal chains ($\epsilon = 0$) to chains with fully developed excluded volume ($\epsilon = \infty$). We let $\beta = 1/(kT)$.

It is by now well established that the partition function of random walks with well-developed excluded volume obeys a relationship of the form²⁻⁴

$$C = ay^N N^{\gamma-1} = ay^N N^\alpha \quad (3)$$

Here a is a model-dependent parameter near unity; y , the "connectivity constant", is also model-dependent, while α is a universal exponent dependent only on the dimensionality of space. N is the number of bonds in the walk. We therefore expect Domb-Joyce lattice walks to obey eq 3 whenever N and w are sufficiently large; in such an instance, we expect both a and y to be functions of w .

We have employed umbrella sampling techniques⁵ to compute the partition function of Domb-Joyce chains on the simple cubic lattice over the entire range of $0 \leq w \leq 1$ and of length up to $N = 500$. The computational technique employed is explained in the next section.

As described above, we expect eq 3 to predict the partition function whenever N and w are sufficiently large, treating y and a as functions of w . Note that by setting $a = 1$, $y = 6$, and $\alpha = 0$, eq 3 also gives the partition function of ideal random walks, i.e., in the extreme that $w = 0$. Given this fact, we have attempted to fit eq 3 to our data over the complete range of w , letting a , y , and α all depend on w . These fits are presented and discussed in the third section. Discrepancies occur in the derivative of the free energy with respect to w when w is near 0, which indicates that eq 3 is not entirely appropriate to the cross-over region. Discrepancies in the derivative of the free energy also occur for small N . Nevertheless, to within

the precision of these calculations, the free energy itself is adequately represented at all values of w by eq 3.

Computational Details

The algorithm that we employed to compute the partition function is one example of the umbrella sampling technique.⁵ In this section we explain in detail the calculational procedure.

Consider a sequence of w_j values in the interval $[0, 1]$: $0 = w_0 < w_1 < w_2 \dots < w_M = 1$. Each one of these defines a Domb-Joyce model chain of steadily increasing excluded-volume strength. Associated with each one of these models is a Hamiltonian, given by eq 1, which we now denote H_j . We also define modified Hamiltonians:

$$H'_j = H_j + B_j \quad (4)$$

B_j is a constant for all elements of the ensemble and may be assumed for the time being to be arbitrary; the motivation for writing these modified Hamiltonians will become apparent shortly. Since B_j is constant, it only shifts the zero point of the energy, and its effects can be easily removed a posteriori. Let C'_j and C_j represent the partition functions evaluated over the Hamiltonians H'_j and H_j , respectively. Then C'_j and C_j differ by a factor $\exp(\beta B_j)$.

We now consider an augmented configuration space by introducing one additional "configurational" variable, σ , which can assume any of the values 0, 1, 2, ..., M . Points in this augmented configuration space are specified by giving the orientations of each of the N bonds in the walk and by giving the value of σ . We define the following Hamiltonian in this augmented space:

$$\mathcal{H} = \sum_{j=0}^M H'_j \delta_{j\sigma} \quad (5)$$

which is to say that $\mathcal{H} = H'_j$ if $\sigma = j$. Let $p_j = \langle \delta_{j\sigma} \rangle$ represent the probability that σ takes the value j when evaluated over the Hamiltonian of eq 5. It is easy to show that p_j is proportional to C'_j :

$$p_j = C'_j / [\sum_j C'_j]^{-1} \quad (6)$$

We can perform Monte Carlo calculations in this augmented configuration space to estimate values of p_j , and since C'_0 is known, we can estimate each of the C'_j partition functions.

For this approach to work, the B_j values must be adjusted so that the C'_j partition functions are all approxi-

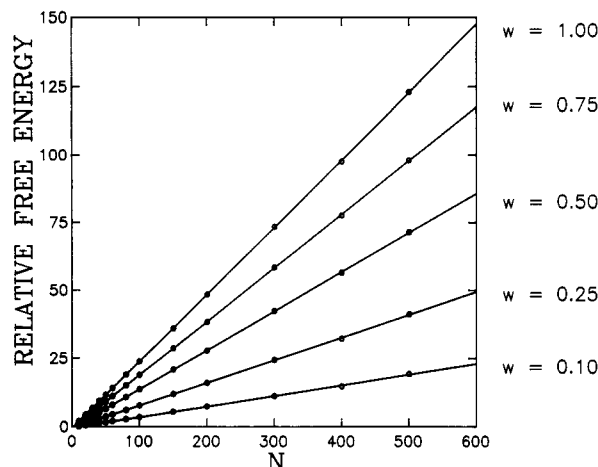


Figure 1. Representative fits of the simulation data to eq 7. The free energies are displayed relative to the free energy of the ideal chain for the values of w indicated.

mately equal. If not, the algorithm would spend all its time at those values of σ for which C_σ' is large and would not adequately sample all values of σ . We were able to obtain adequate B_j values either by trial and error in relatively short preliminary computer runs or by extrapolation or interpolation from previous results. Once adequate B_j values were obtained, refined values of the partition functions C_j were obtained in longer production runs.

For the technique to work it is also necessary that each w_j be fairly close to w_{j+1} . If not, transitions in σ will occur infrequently. In our calculations, we found it adequate to set $w_j = j/100$, with $M = 100$.

In the calculations with large values of N , we found that the time required for σ to "diffuse" from values near 0 to values near M was excessively long. Therefore, in all the calculations with $N \geq 300$, the calculation was broken up into overlapping smaller calculations. The first included H_j' hamiltonians 0 through 20, the second 10 through 30, etc.

The walk through configuration space followed this procedure:

1. Randomly select a new σ value; $\sigma' = (\sigma \pm 1) \bmod M$.
2. Randomly select an integer I in the interval $[-1, N]$, where N is the total number of steps in the walk.
3. If $I = -1$, erase the first bond of the walk and redraw it with random orientation.
4. If $I = 0$, erase bonds 1 and 2 and then redraw them in arbitrary orientations.
5. If $I = N$, erase the N th bond of the walk and then redraw it at random.
6. If $I = N - 1$, erase bonds $N - 1$ and N and then redraw them at random.
7. For all other values of I , first determine the vector sum of the three bonds I , $I + 1$, and $I + 2$. Let \mathbf{V} be the name of this vector. Now erase these three bonds. Randomly select new orientations for these three bonds from a table (generated previously and stored in main memory) listing all possible three-bond sequences that sum up to the vector \mathbf{V} .
8. Calculate the change in energy according to eq 5 and accept the new position conditionally by the usual Metropolis criterion.⁶

Results

The free energy of simple cubic lattice polymers was calculated according to the procedure explained above, at values of the Domb-Joyce parameter $w = 0.00, 0.01, 0.02, \dots, 1.00$ and at the chain length values $N = 10, 20, 30, 40,$

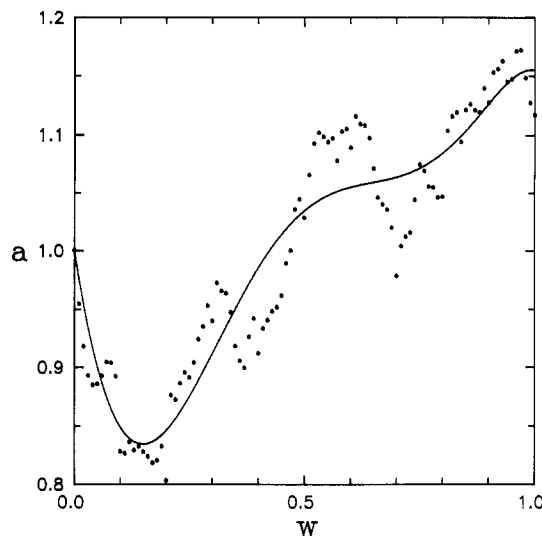


Figure 2. Best-fit values of the amplitude a (circles) and the sixth-order polynomial approximation to these values (solid curve).

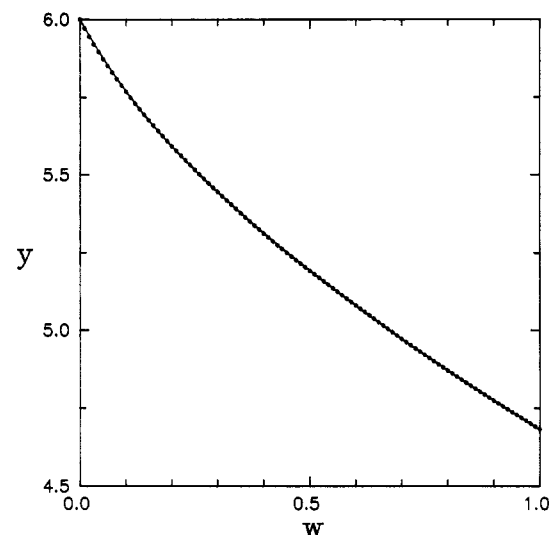


Figure 3. Best-fit values of the connectivity constant (circles) and the sixth-order polynomial approximation to these values (solid curve).

50, 60, 80, 100, 150, 200, 300, 400, and 500. All the data points at a given value of w were then fit to an equation having the form of eq 3:

$$\beta A = -\ln a - N \ln y - \alpha \ln N \quad (7)$$

Here A represents the free energy and β is $1/kT$. Least-squares best-fit values of $\ln a$, $\ln y$, and α were obtained at each value of w . Figure 1 displays fits for several values of w , plotted as the free energy relative to the ideal chain, $\beta A + N \ln 6$. Figures 2-4 display the best-fit values of a , y , and α as functions of w . The term in $\ln y$ dominates eq 7, and so it comes as no surprise that Figure 3 displays much less noise than either Figure 2 or 4. The noise level in Figures 2 and 4 indicates that βA has been determined to a precision of about ± 0.1 or 0.2 .

We note that the connectivity constant $y(w)$ has been determined rather accurately in these simulations. At $w = 1$ we have obtained $y = 4.68$, as expected.^{3,4,7} The exponent α levels off, as expected, at a value of about 0.18, in good agreement with the second-order ϵ -expansion value of 0.176.⁴

Motivated by the desirability of empirical functional relationships for the free energy, we have done least-

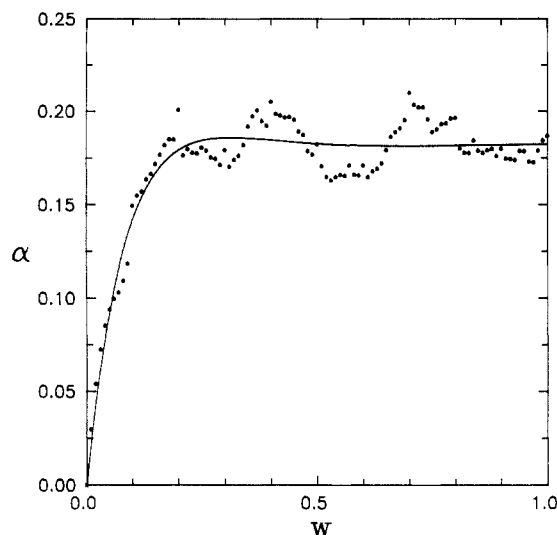


Figure 4. Best-fit values of the exponent α (circles) and the approximation to these values (solid curve).

Table I
Best-Fit Coefficients a_j , y_j , and α_j

j	a_j	y_j	α_j
0	1.0000	6.0000	0.0000
1	-2.5404	-2.6823	2.1670
2	11.722	4.3637	-3.7235
3	-13.712	-7.1360	1.2158
4	-7.0006	6.8704	1.8833
5	21.964	-3.3447	-0.5234
6	-10.278	0.6094	-0.6640

squares fits of the following functions to the data shown in Figures 2-4:

$$a(w) = \sum_{j=0}^6 a_j w^j \quad (8)$$

$$y(w) = \sum_{j=0}^6 y_j w^j \quad (9)$$

and

$$\alpha(w) = \sum_{j=1}^6 \alpha_j [(w + 0.9)^{-j} - 0.9^{-j}] \quad (10)$$

The values of the coefficients a_j , y_j , and α_j obtained are given in Table I. The solid curves in Figures 2-4 display the least-squares fits. Of course, given the level of uncertainty in $a(w)$ and $\alpha(w)$, eq 8 and 10 are probably rather crude representations of the true functions. However, as Figure 3 shows, eq 7 is probably a good representation of the dominant term, $y(w)$. The fits were all constrained to pass through the known values of a , y , and α at $w = 0$, which is achieved by requiring $a_0 = 1$, $y_0 = 6$, and $\alpha_0 = 0$.

We now examine how closely the empirical fit, given by eq 7-10, reproduces the simulation data. To do this, we define the least significant part of the free energy per bond as

$$T = \beta A/N + \ln y = -(\ln a + \alpha \ln N)/N \quad (11)$$

and plot values of T in Figures 5 and 6. The symbols in Figures 5 and 6 are drawn at the points $\beta A/N + \ln y$ with βA taken from the simulation data and y calculated according to eq 9. The solid curves are loci of the functions $-(\ln a + \alpha \ln N)/N$ with a and α calculated according to eq 8 and 10. The primary conclusion that we can draw from Figures 5 and 6 is that the empirical fit for βA and the simulation data for βA usually agree within about 0.1

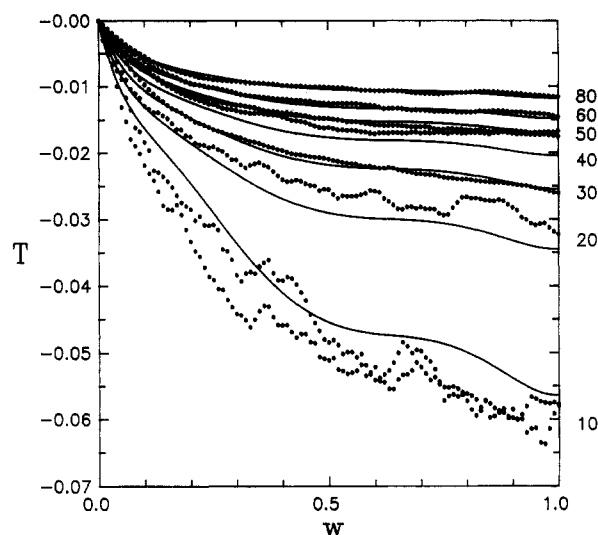


Figure 5. Comparison between the nondominant part (defined as T in eq 11) of the simulated free energy per bond (symbols) and the empirical fit (solid curves), for the values of N given on the right.

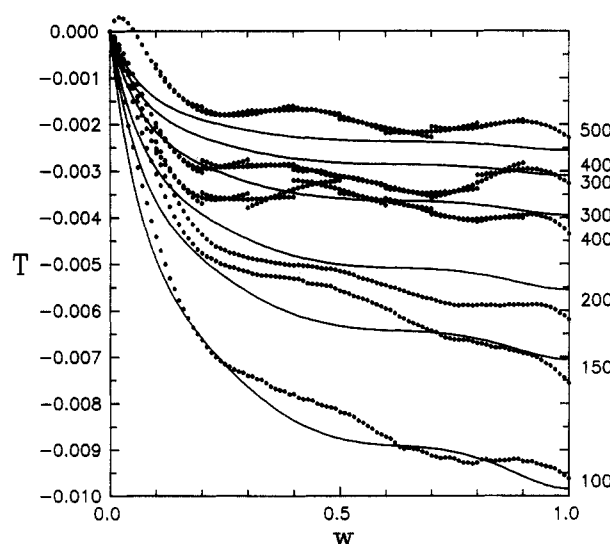


Figure 6. Comparison between the nondominant part (defined as T in eq 11) of the simulated free energy per bond (symbols) and the empirical fit (solid curves), for the values of N given on the right. Because of sampling errors, the simulated data for $N = 300$ lie above those for $N = 400$.

or 0.2. (E.g., the level of discrepancy in T for $N = 500$ is about 0.0005; this translates into a discrepancy of 0.25 in βA itself.)

We now examine how well the empirical fit, eq 7-10, predicts the first derivative of the free energy, which determines, of course, quantities such as the energy and entropy. Let $\langle c \rangle$ represent the average number of pairwise contacts at given values of w and N . It also is given by the first derivative of the free energy:

$$\langle c \rangle = (1 - w) \frac{\partial(\beta A)}{\partial w} \quad (12)$$

During the course of the simulation, we also accumulated statistics on the number of pairwise contacts. Figure 7 displays a comparison between the simulated $\langle c \rangle/N$ values and those calculated according to eq 7-10 and 12. The fit is rather poor at small N but is quite good at larger N except near $w = 0$.

To further investigate the behavior of the fit at small w , we have computed the free energy to first order in w

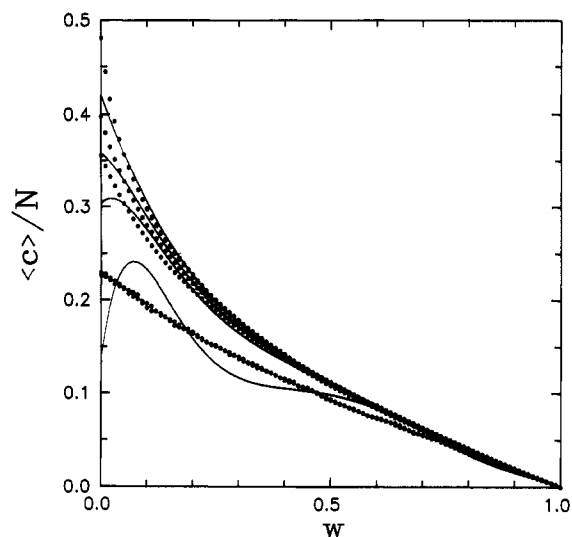


Figure 7. Average number of pairwise contacts per backbone bond versus w . The circles are simulation data; the solid curves are derived from the empirical fit. Only the $N = 10, 50, 100$, and 500 curves are shown and occur in ascending order.

by perturbation theory, as discussed in the Appendix. This yields, of course, the first derivative of βA at $w = 0$, and it follows that we can write

$$\langle c \rangle / N = 0.51847 - 1.3087N^{-1/2} + 1.3509N^{-1} \quad \text{at } w = 0 \quad (13)$$

Equation 13 is valid to better than 1% at all values of $N \geq 20$ and so for our purposes is essentially exact. Compare this with the approximation obtained through the use of eq 7:

$$\langle c \rangle / N \cong -y_1/y_0 + QN^{-1} \ln N - (a_1/a_0)N^{-1} \quad \text{at } w = 0 \quad (14)$$

where

$$Q = \sum_{j=1}^6 j \alpha_j (0.9)^{-j-1} = -2.4772 \quad y_1/y_0 = -0.4470 \quad (15)$$

$$a_1/a_0 = -2.5404$$

Figure 8 compares these two expressions for $\langle c \rangle / N$ at $w = 0$ with the simulation data. The exact series, eq 13, agrees well with the simulation results, while the approximation is consistently lower. Obviously, we could obtain better agreement in Figure 8 by constraining y_1/y_0 to be -0.51847 , while allowing the other y_j to adjust accordingly, thereby constraining eq 14 to agree asymptotically with eq 13 and shifting the associated curve in Figure 8 upward. We made such an attempt but found in so doing that the overall fit at larger values of w worsened. Therefore, we prefer to retain the y_j values given in Table I and sacrifice accuracy in $\partial(\beta A)/\partial w$ at small w for a generally improved fit at all other values of w .

Equations 13 and 14 are particular examples of general properties of random walks. For w near zero, the subdominant term in the free energy or its derivatives is proportional to $N^{1/2}$, while for larger w , it is proportional to $\ln N$. Therefore, one should not expect eq 3 to apply in the cross-over region. That it is successful at all is attributable to two facts: first, that the dominant term in the free energy is proportional to N in all cases and, second, that $N^{1/2}$ and $\ln N$ have vaguely comparable forms. (Both are monotone increasing with steadily decreasing slopes. Figure 8 with a vertical shift of one of the curves relative to the other demonstrates the degree to which the functions $N^{1/2}$ and $N^{-1} \ln N$ are superimposable.)

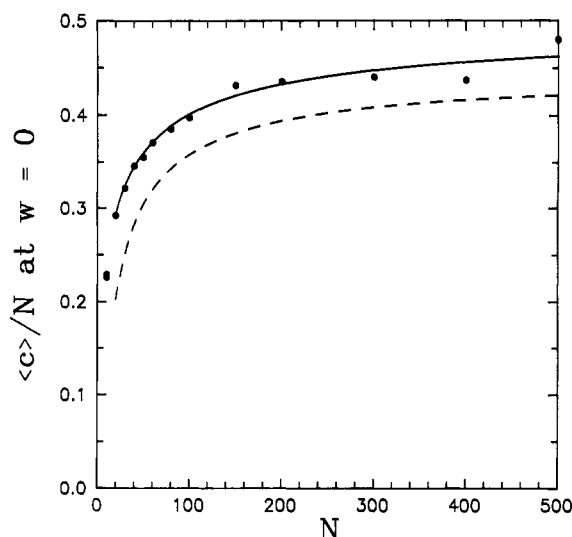


Figure 8. Average number of pairwise contacts per bond in the ideal chain (i.e., at $w = 0$) versus the number of bonds. Shown are the simulation data (filled circles); the exact expression, eq 13 (solid curve); and the approximation provided by the empirical fit, eq 14 (dashed curve).

Conclusions

Through umbrella sampling techniques we have computed the free energy of simple cubic lattice chains that experience a Domb-Joyce excluded-volume interaction over the complete range of excluded-volume interaction. The data are rather well represented by eq 7-10, to a precision of about ± 0.2 kT. These results provide an accurate calculation of the connectivity constant for all values of the excluded-volume strength (Figure 3 and eq 9). The critical exponent $\gamma - 1 = \alpha$ is computed to about 0.18.

Appendix. Perturbation Expansion of the Free Energy

Elegant generating function techniques exist for the development of perturbation expansions of the free energy and other properties of lattice walks in powers of w .^{1,8,9} Given the existence of these techniques, the authors are chagrined to report the following sledgehammer approach that they employed to generate the first-order perturbation expansion of the free energy.

Let $\nu \in \{1, 2, 3, \dots, 6^N\}$ index all the N -step random walks on the simple cubic lattice. The energy of the ν th random walk is

$$U_\nu = \epsilon \sum_{i < j} \delta_{ij}^\nu \quad (A1)$$

where δ_{ij}^ν is 0 if the i th and j th beads of the ν th walk do not coincide, and it is 1 if they do. The above sum simply counts all the pairwise contacts within the ν th chain. The partition function is given, therefore, as

$$C = \sum_\nu \prod_{i < j} \exp[-\beta \epsilon \delta_{ij}^\nu] \quad (A2)$$

Recalling the definition of w in eq 2 above, the partition function may also be written

$$C = \sum_\nu [1 - w \sum_{i < j} \delta_{ij}^\nu] + O(w^2) \quad (A3)$$

Now the following summation is just the number of random walks for which beads i and j overlap

$$c_{ij} = \sum_\nu \delta_{ij}^\nu \quad (A4)$$

but since each step of the walk is entirely random, this is just

$$c_{ij} = 6^{N+i-j}\Gamma_{j-i} \quad (\text{A4}')$$

where we let Γ_n represent the number of unique closed paths of length n on the lattice. It follows that

$$C = 6^N[1 - w\sum_{i < j} 6^{i-j}\Gamma_{j-i}] + O(w^2) \quad (\text{A5})$$

and therefore, that the free energy is given by

$$\beta A = -N \ln 6 + w\sum_{i < j} 6^{i-j}\Gamma_{j-i} + O(w^2) \quad (\text{A6})$$

or

$$\beta A = -N \ln 6 + w\sum_{p=1}^N (N-p+1)6^{-p}\Gamma_p + O(w^2) \quad (\text{A7})$$

Γ_n can be calculated combinatorially; the result is

$$\Gamma_n = \sum_{\{n_1, n_2, n_3\}} \frac{n!}{(n_1!)^2(n_2!)^2(n_3!)^2} \quad (\text{A8})$$

where $\sum_{\{n_1, n_2, n_3\}}$ indicates a sum over all possible values of n_1 , n_2 , and n_3 such that n_1 , n_2 , and n_3 are nonnegative integers and $2(n_1 + n_2 + n_3) = n$. (Γ_n is zero for odd n .) The above calculations are almost trivial for today's tireless computers, and using eq A7 and A8 we were able to obtain accurate values for the quantity Q_N in the expansion

$$A = -N \ln 6 + Q_N w + O(w^2) \quad (\text{A9})$$

It has been established^{8,9} that each coefficient such as Q_N in eq A9 can be written as a power series in $N^{-1/2}$; via a straightforward least-squares fit we have obtained:

$$Q_N = 0.51847N - 1.3087N^{1/2} + 1.3509 \quad (\text{A10})$$

Equation 10 is valid with a precision of better than 1% whenever $N \geq 20$. This leads directly to eq 13.

Acknowledgment. We express gratitude to the National Science Foundation (Grant DMR-8607708) and to the Michigan Polymer Consortium (Award 001) for partial support of this research.

References and Notes

- (1) Domb, C.; Joyce, G. S. *J. Phys. C* **1972**, *5*, 956.
- (2) Freed, K. F. *Renormalization Group Theory of Macromolecules*; Wiley-Interscience: New York, 1987.
- (3) de Gennes, P.-G. *Scaling Concepts in Polymer Physics*; Cornell University Press: Ithaca, NY, 1979.
- (4) Cherayil, B. J.; Douglas, J. F.; Freed, K. F. *Macromolecules* **1987**, *20*, 1345.
- (5) Valleau, J. P.; Torrie, G. M. In *Statistical Mechanics A: Equilibrium Techniques*; B. J. Berne, Ed.; Plenum: New York, 1977.
- (6) Valleau, J. P.; Whittington, S. G. In *Statistical Mechanics A: Equilibrium Techniques*; Berne, B. J., Ed.; Plenum: New York, 1977.
- (7) Gaunt, D. S. *J. Phys. A* **1986**, *19*, L149.
- (8) Barrett, A. J.; Domb, C. *Proc. R. Soc. London A* **1979**, *367*, 143.
- (9) Barrett, A. J.; Domb, C. *Proc. R. Soc. London A* **1981**, *376*, 361.

Θ Temperature of Ring Polymers: Another Evidence of Topological Interaction

Kazuyoshi Iwata

Faculty of Engineering, Fukui University, Bunkyo 3, Fukui 910, Japan.

Received December 7, 1988; Revised Manuscript Received February 23, 1989

ABSTRACT: Roovers and Toporowski (RT) have found that ring polystyrene (PS) in cyclohexane has a fairly large A_2 at the Θ temperature of the corresponding linear polymer, Θ ; and the Θ temperature of the ring, Θ_r , is remarkably lower than that of the linear polymer. This abnormality is considered to come from the topological repulsion among the ring polymer molecules. The nonzero A_2 observed at Θ is called "topological second virial coefficient A_2^{top} ", which has been studied in the previous work. In the present paper, the excluded-volume potential is introduced into the previous theory, and the Θ temperature difference $\Delta\Theta$ ($=\Theta_r - \Theta$) is computed for various ring polymers and solvents; for ring PS in cyclohexane, the computed results agree well with the experiments of RT. It is predicted that $\Delta\Theta$ is inversely proportional to the temperature coefficient of the binary cluster integral among segments, and in some systems (say, PS in diethyl malonate and 1-chloro-*n*-undecane), $\Delta\Theta$ is as large as 20° . It is argued that dilute solutions of ring polymer are the most fundamental system for studying polymer entanglement.

Introduction

Entanglement of polymers is usually discussed in terms of the tube model.¹ This model has succeeded in explaining the viscoelastic properties of entangled polymer systems very well,¹ but its application has been limited mainly to dynamic properties. It is recently considered that entanglement plays an important role in much broader properties of polymers, such as rubber elasticity^{3,4} or solution properties of ring polymers.^{2,5,6} It is, however, difficult to apply the tube model to these problems in a reasonable way, and a more fundamental approach must be taken to study them. Entanglement is more adequately described by introducing topological invariants such as the Gauss integral explicitly into the statistical mechanics of polymer molecules. From this consideration, we have been developing "topological theories of entanglement" to cover

broader fields of entanglement, such as dynamics of linear polymers,⁷ solution properties of ring polymers,^{2,5} and elastic properties of network³ and linear⁸ polymers. These theories are constructed systematically so that entanglement of the all systems is characterized by single molecular parameter called the "topological interaction parameter $\bar{\gamma}$ ", which represents how strongly polymer molecules can entangle with each other. The present paper is a part of this series.

A dilute solution of a ring polymer is the simplest system in which the topological interaction exists. This system is particularly interesting in the study of entanglement, because its physical properties can be measured more accurately and their theoretical calculation is easier than in other entangled systems. Roovers and Toporowski (RT)^{9,10} have found that ring polystyrene in cyclohexane